ANALYTICAL SCIENCES AUGUST 2017, VOL. 33

Christmas-tree Derived Amplification Immuno-strategy for Sensitive Visual Detection of *Vibrio parahaemolyticus* Based on Gold Label Silver Stain Technology

Xinxin Song,* Yanjie Wu,* Lin Wu,* Yufang Hu,* Wenrou Li,* Zhiyong Guo,*† Xiurong Su, and Xiaohua Jiang*****

**Faculty of Materials Science and Chemical Engineering, Ningbo University, Ningbo 315211, PR China*
***School of Marine Sciences, Ningbo University, Ningbo 315211, PR China*
****School of Applied Chemistry and Biological Technology, Shenzhen Polytechnic, Shenzhen 518055, PR China*

A developed Christmas-tree derived immunosensor based on a gold label silver stain (GLSS) technique was fabricated for a highly sensitive analysis of *Vibrio parahaemolyticu* (VP). In this strategy, captured VP antibody (cAb) was immobilized on a solid substrate; then, the VPs were sequentially tagged with a signal probe by incubating the assay with a detection VP antibody (dAb) conjugated gold nanoparticles (AuNPs)-labeled graphite-like carbon nitride (g-C_3N_4). Finally, the attached signal probe could harvest a visible signal by the silver meal deposition, and then followed by homebrew Matlab 6.0 as a grey value acquisition. In addition, the overall design of the biosensor was established in abundant AuNPs and g-C_3N_4 with a two-dimensional structure, affording a bulb-decorated Christmas-tree model. Moreover, with the optimized conditions, the detection limit of the as-proposed biosensor is as low as 10^2 CFU (Colony-Forming Units) mL^{-1}, exhibiting an increase of two orders of magnitude compared with the traditional immune-gold method. Additionally, the developed visible immunosensor was also successfully applied to the analysis of complicated samples.

Keywords Immunosensor, *Vibrio parahaemolyticus*, gold label silver stain technology, AuNPs@g-C_3N_4

(Received February 3, 2017; Accepted April 4, 2017; Published August 10, 2017)

Introduction

Vibrio parahaemolyticus (VP), a gram-negative halophilic bacterium, is one of the important marine seafood-pathogens with a natural distribution in coastal marine estuarine environments.[1,2] Infections commonly from the consumption of raw or partially cooked seafood, may lead to symptoms including headache, vomiting, nausea, low-grade fever, and sometimes fatal infections.[3,4] Current epidemiological data show that VP has become a focus of food safety in Asia, South America and United States, while VP was first recognized as a cause of food-borne diseases in Osaka, Japan in 1951.[5-7] Although conventional culturing ensures the accuracy of determinations, and are optimum methods for VP identification, there still exist some shortcomings, such as long-time consumption and cumbersome practical application. Various approaches have been developed to obtain better performances of VP analysis, including enzyme-linked immunesorbent assay (ELISA),[8-10] DNA probe,[11] most probable number (MPN),[12,13] polymerase chain reaction (PCR),[14-18] loop-mediated isothermal amplification (LAMP),[19-23] and electrochemistry (EC).[24,25] Despite each of these new approaches having a combination of excellent sensitivity, accuracy and specificity, they still suffer drawbacks involving high analytical cost, need for expensive equipment, and professional trained personnel. Therefore, simple, rapid, sensitive and low-cost assays for determining VP are urgently needed.

Gold nanoparticles (AuNPs), which have unique physical and chemical properties including rapid and easy synthesis, efficient surface-area-to-volume ratios, non-toxicity, and desirable biocompatibility,[26-28] are very attractive labels in the biomedical field, and display extreme scattering cross sections and strong absorption. In addition, the gold label silver stain (GLSS) technique is commonly used in conjunction with visible detection like DNA,[29] proteins[30] and bacteria.[31] AuNPs can not only act as gray value harvesting antennae for dye by means of metallic silver, which is produced by a catalytic reduction of silver ions, but also can serve for an excellent substrate carrier, and thus facilitate the precipitation of silver. It thus provides probability of a highly sensitive, simple and visual method for VP detection in seawater and seafood.

Graphite-like carbon nitride (g-C_3N_4), as a two-dimensional structure material, has novel properties, such as wear resistance, chemical inertness, high hardness and exhibits excellent performance in the photocatalysis fields,[32] photoelectronic devices,[33] and chemical sensors.[34] Recently, g-C_3N_4/metal nanoparticles composites have aroused extensive interest.[35] Li *et al.* reported on the synthesis of Ag@g-C_3N_4 to construct a highly sensitive immunosensing.[36] Recently, Liu and his co-workers designed a Fe(III)-grafted g-C_3N_4 photocatalyst that displayed an excellent photocatalytic performance.[37] These make it promising in the development of biosensors with high

† To whom correspondence should be addressed.
E-mail: guozhiyong@nbu.edu.cn

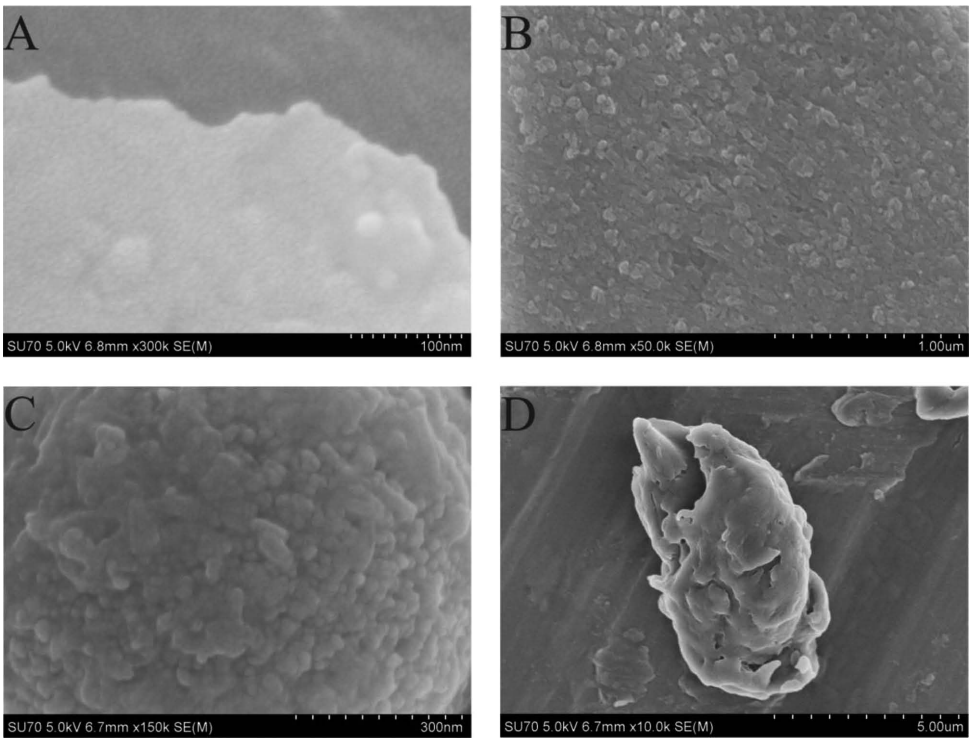

Fig. 1 SEM image of (A) g-C_3N_4, (B) AuNPs@g-C_3N_4, (C) dAb-AuNPs@g-C_3N_4 and (D) VP- dAb-AuNPs@g-C_3N_4.

performances. Moreover, very few reports on g-C_3N_4-revelent nano-materials are available in literature regarding the gray valve-derived bacteria detection platform.

Herein, this study presents a novel and highly sensitive Christmas-tree-like immunosensor for the detection of VP based on AuNPs@g-C_3N_4 signal amplification and visible strategy. In this strategy, an extraordinary sandwich assay was used *via* the interaction of antigen and antibody: firstly, the cAb was irreversibly fixed on silanized slides to capture VP; secondly, the dAb-AuNPs@g-C_3N_4 was assembled by VP, followed by silver staining. The proposed method does introduce g-C_3N_4 to carry more signal units, making it more applicable for low-detection. With this proposed method, it exhibits good linear response from 10^2 to 10^7 CFU mL^{-1} with a detection of VP as low as 10^2 CFU mL^{-1}, which was 2 orders of magnitude more sensitive than the traditional GLSS assay. Furthermore, it was successfully applied to the direct determination of VP in seawater and seafood simultaneously.

Experimental

Reagents and chemicals

The Silver Enhancer Kit consisting of solution A (silver salt), solution B (initiator), (3-aminopropyl) triethoxysilane (APTES) and 2.5% glutaraldehyde solution was purchased from Sigma-Aldrich (St. Louis, USA). Polyclonal *Vibrio parahaemolyticus* (VP) antibody, using as capture antibody (cAb) and detection antibody (dAb), were obtained from Sangon Biotech Co., Ltd. (Hangzhou, China). Melamine, hydrogen tetrachloroaurate(III) hydrate ($HAuCl_4{\cdot}4H_2O$) and sodium citrate were purchased from Sinopharm Reagent Co., Ltd. (Shanghai, China). Milli-Q water (18 MΩ cm) was used in all experiments. All of the other chemicals were of analytical-reagent grade and used without further purification.

Apparatus

The A4 flatbed scanner K820 (BenQ, Beijing, China) was used to obtain clear silver stain signals. The morphologies of prepared nano-materials were characterized with a Hitachi SU-70 scanning electron microscope (SEM, Hitachi, Tokyo, Japan). The silver stain signals on the slide were scanned into gray scale images with a resolution of 1200 dpi. Then, silver spots were picked up by Photoshop CS5, and these data of separate spots were processed by Matlab 6.0 using custom-made program. So, average grey value of silver stain spot was calculated as the summation of grey value.

Synthesis of dAb-AuNPs@g-C_3N_4

The g-C_3N_4 and AuNPs were prepared according to previous literature (in Supporting Information),[38,39] respectively. AuNPs@g-C_3N_4 composites were obtained by Chen's literature.[40] First, 50 mg g-C_3N_4 and 50 mL gold colloidal solution were mixed under gentle stirring for 24 h at room temperature. After that, the resulting solution was centrifuged at 8000 rpm to remove unloaded AuNPs. Finally, the resulting precipitate was re-dispersed into 20 mL of water and stored at 4°C. Figure 1A shows a typical SEM image of pristine g-C_3N_4 that is well known to comprise a lamellar structure of g-C_3N_4 sheets. For AuNPs@g-C_3N_4, SEM image (Fig. 1B) shows that individual AuNPs are homogeneously distributed on the surface of g-C_3N_4 sheet, indicating that AuNPs@g-C_3N_4 was successfully prepared.

As shown in Scheme 1A, the method of conjugation of dAb with AuNPs@g-C_3N_4 is described below. First, 400 µL of 10^{-3} mg mL^{-1} dAb and 400 µL AuNPs@g-C_3N_4 were incubated at 35°C for 4 h. Then, 200 µL of 1 wt% BSA was added to block non-specific adsorption. Finally, the composites of dAb-AuNPs@g-C_3N_4 were obtained after washing and reconstructing in 400 µL of ultrapure water. As shown in Fig. 1C, the surface obviously hunched and the structure of film was completely changed, which indicated that protein molecules such as dAb

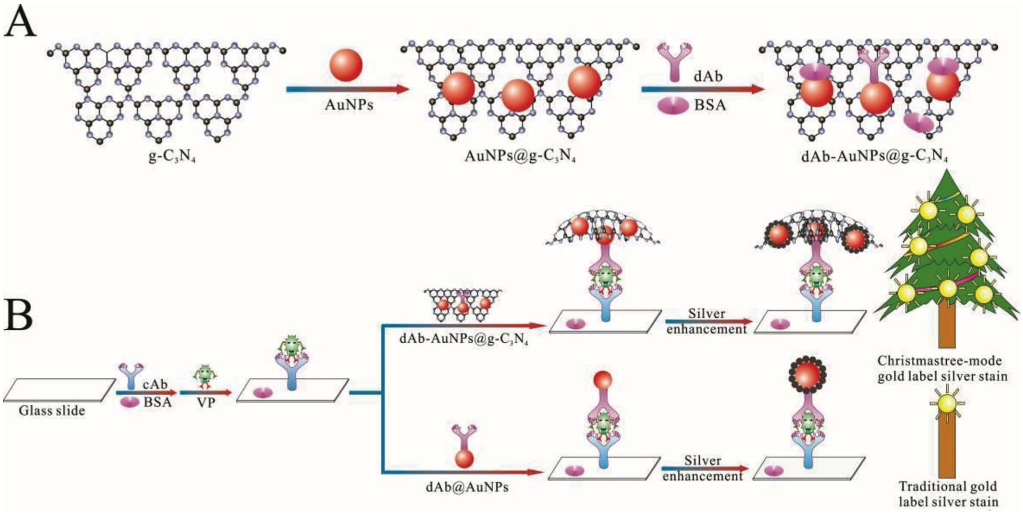

Scheme 1 Schematic illustration for (A) the preparation of dAb-AuNPs@g-C_3N_4 and (B) our Christmas-tree derived GLSS assay compared with traditional one.

and BSA were immobilized on the surface of AuNPs@g-C_3N_4. Simultaneously, Fig. 1D shows the immunoreaction between VP and dAb-AuNPs@g-C_3N_4, manifesting the probe was firmly captured by VP.

Sandwich direct immunoassay

The silanzied slides were used for the detection of VP using a sandwich immunoassay. Firstly, 5 µL 2.5% glutaraldehyde ($C_5H_8O_2$) solution was dripped onto the surface of silanzied slide for 30 min to construct a test zone. Then, 5 µL 10^{-3} mg L^{-1} cAb was added to the test zone and incubated for 60 min. To block the excess aldehyde groups against non-specific binding proteins, the test zone was incubated with 1% BSA and the excess solution was washed away. Secondly, 5 µL VP with different concentrations (10^1, 10^2, 10^3, 10^4, 10^5, 10^6, 10^7, 10^8 CFU mL^{-1}) were incubated over the glass substrate to react with cAb for 30 min and the ultrapure water was used to remove any excess VP solution. Finally, 5 µL dAb-AuNPs@g-C_3N_4 were incubated onto VP for 30 min. Following washing, a silver stain process was carried out as follows. Equal amounts of silver enhancer solution A and solution B were thoroughly added to the mixture, and 5 µL of a mixed enhancer-solution was dripped on the above-mentioned test zone. Then, the slide was immediately placed in the dark to react for 15 min. After that, the silver solution was discarded to terminate the reaction. Finally, the slides were washed with ultrapure water and air-dried at room temperature.

Results and Discussion

Principle

Scheme 1A describes the configuration of the Christmas-tree-like immunosensor for VP visible detection. The g-C_3N_4 was used as a supporter to load a large quantity of AuNPs *via* electrostatic adsorption.[40] Then, with the addition of dAb, the resulting dAb-AuNPs@g-C_3N_4 provides a platform for sensitively assaying VP *via* a sandwich immunoassay, including immobilization of cAb, immunoreaction on the prepared slide surface. It is well known that silver metal is deposited by AuNPs, and is always accompanied with black silver stain signals, which can be seen by the naked eye.[41,42] In traditional immunogold assays (Scheme 1B), the results are easily influenced by the density of AuNPs. Limited binding sites on dAb are used for AuNPs, resulting in one target corresponding to limited AuNPs. But, in this study (Scheme 1B) the new functional conjugation strategy is more sensitive due to the application of AuNPs@g-C_3N_4. Hence, it ensures one target is corresponding to large number of AuNPs. Most importantly, these bounding AuNPs are to become signal units and be enlarged by silver metal deposition. Therefore, the proposed method will bring benefits for improving of the sensitivity and reliable lower detection limit.

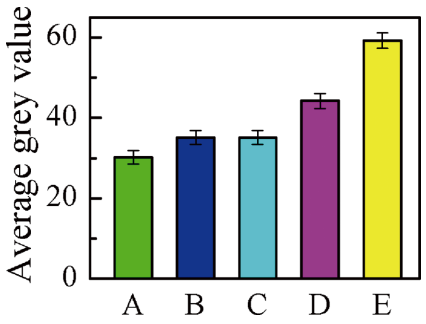

Fig. 2 Feasibility of a Christmas-tree derived immunoassay sensor by investigating different samples: (A) dAb (B) dAb + silver stain, (C) dAb + g-C_3N_4 + silver stain, (D) dAb + AuNPs + silver stain, (E) dAb + AuNPs@g-C_3N_4 + silver stain. VP concentrations was 10^4 CFU mL^{-1}.

Feasibility analysis of the Christmas-tree derived immunosensor

To prove the validity of the Christmas-tree derived immunoassay sensor, five sets of dAb content were tested: (A) dAb, (B) dAb + silver stain, (C) dAb + g-C_3N_4 + silver stain, (D) dAb + AuNPs + silver stain, (E) dAb + AuNPs@g-C_3N_4 + silver stain, respectively. As shown in Fig. 2, comparing A with B, the average grey value in B slightly increased with the silver stain because few silver ions were reduced. No significant difference was observed between C and B, implying that the grey value does not increase when g-C_3N_4 is used alone. However, with the addition of AuNPs@g-C_3N_4 into the dAb solution (E), the grey value was obviously increased in

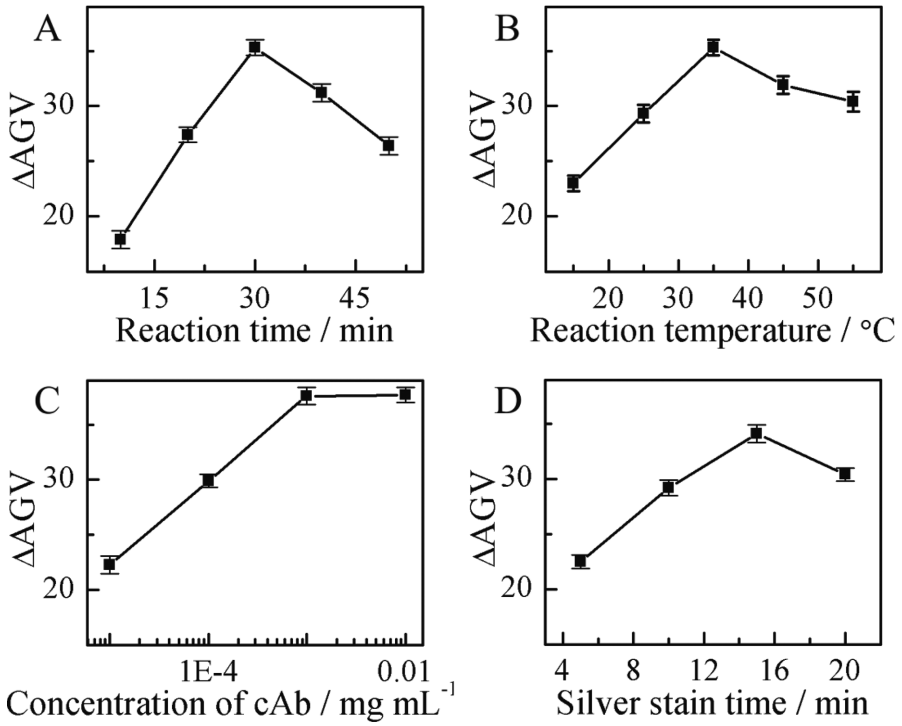

Fig. 3 Optimization of (A) reaction time, (B) reaction temperature, (C) concentration of cAb and (D) the silver stain time on ΔAGV.

comparison with other experiments (C, D), suggesting the signal can be greatly amplified by AuNPs@g-C_3N_4. Those observations indicate that it is reasonable that the formation of a Christmas-tree derived immunoassay sensor holds great potential for use in the detection of VP.

Optimization of experimental conditions

Obviously, the average grey value was greatly influenced by (i) the reaction time between VP and dAb, (ii) the reaction temperature, (iii) the concentration of cAb, and (iv) the reaction time on silver stain. To study the optimal experimental conditions mentioned above, 10^6 CFU mL^{-1} of VP samples were prepared. For comparing expediently and intuitively, the reduced average grey value (ΔAGV) here was introduced, which is defined as the average grey value in the presence of VP at a certain concentration minus the average grey value in the absence of VP. The effect of reaction time between VP and dAb on ΔAGV is presented in Fig. 3A. ΔAGV increased and reached a maximum value at 30 min, then decreased. The reason is as follows. The average grey value in the presence of VP at a certain concentration increased with the reaction time, while the average grey value in the absence of VP caused by nonspecific adsorption also increased with the reaction time. The maximum ΔAGV could be obtained at 30 min, which could bring the highest sensitivity. Therefore, 30 min was selected as the optimal reaction time.

The effect of the reaction temperature on the ΔAGV was also investigated. As shown in Fig. 3B, the ΔAGV increased with the increment of reaction temperature until a maximum value reached at 35°C. Therefore, the reaction temperature of 35°C was selected for the immunoassay.

The concentration of cAb was taken into consideration, as shown in Fig. 3C; the ΔAGV increased with increasing the concentration of cAb, and reached a constant value of 10^{-3} mg mL^{-1}. The ΔAGV increased with the increase of the sliver stain time and gradually decreased when it was over 15 min (Fig. 3D), since the grey value of background increased once further prolonging the reaction time. Therefore, the optimal reaction time between VP and dAb, reaction temperature, the concentration of cAb and sliver stain time for higher sensitivity were 30 min, 35°C, 10^{-3} mg mL^{-1} and 15 min.

Linearity and sensitivity

As a comparison, the traditional assay and enhanced GLSS assay were simultaneously performed; the results are shown in Fig. 4. The relationship between the average grey value and VP concentrations was discussed (Figs. 4A and 4B). For the proposed method in this study, the linear range was from 10^2 to 10^7 CFU mL^{-1}, and the limit of detection of VP was as low as 10^2 CFU mL^{-1}. The regression equation was expressed as $y = 27.21 + 7.97 \times \log x$ (CFU mL^{-1}) with a correlation coefficient of 0.996. However, the traditional assay shows a narrow linear range from 10^4 to 10^7 CFU mL^{-1}, and the regression equation was $y = 28.15 + 4.01 \times \log x$ (CFU mL^{-1}) with a correlation coefficient of 0.994. The traditional method could achieve the detection of VP as low as 10^4 CFU mL^{-1}. The corresponding spot images are shown in Fig. 4C (proposed method) and Fig. 4D (conventional one), revealing that the grey scale increased with increasing concentration of VP. The sensitivity of the proposed method is as low as 10^2 CFU mL^{-1}, which is 2 orders of magnitude higher than traditional immune-gold method. Such a high sensitivity is due to two reasons: (1) GLSS method itself is a highly sensitive method; (2) a Christmas-tree derived amplified strategy is constructed to amplify signal.

As compared with other approaches reported, there are some special advantages to this proposed method, as shown in Table 1. Firstly, it exhibits a low detection limit, which is nearly the same as or much lower than those reported values of 7.374×10^4 CFU mL^{-1},[8] 112 CFU g^{-1},[17] 87 CFU g^{-1},[20] and 1.7 CFU g^{-1}.[25]

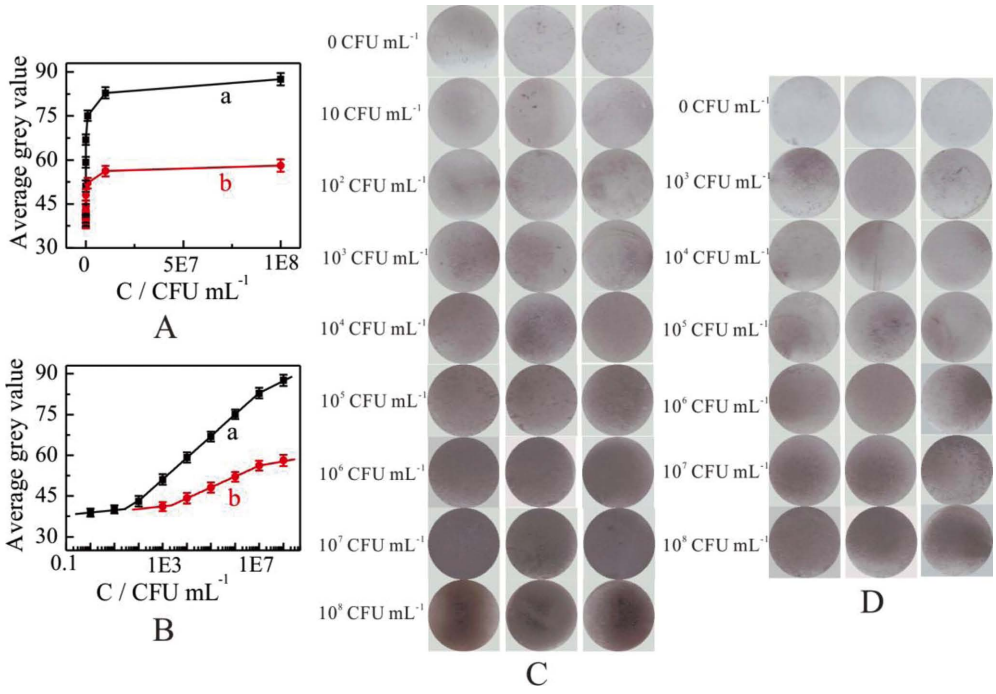

Fig. 4 Linearity and sensitivity of the assay. The average grey value of spot images as a function of (A) VP concentrations and (B) the logarithm of VP concentrations by Christmas-tree derived method (curve a) and traditional method (curve b); spot images of VP at various concentrations by using (C) Christmas-tree derived method and (D) traditional method.

Table 1 Comparison of the main methods reported for the determination of VP

Analytical method	Sample	Detection time/h	LOD	Reference
ELISA	Shrimp	0.5	7.4×10^4 CFU mL^{-1}	8
PCR	Shrimp	0.83	112 CFU g^{-1}	17
	Shellfish	6	100 CFU mL^{-1}	18
LAMP	—	2	10 CFU mL-1	19
	Shellfish	4	87 CFU g^{-1}	20
Immuno-fluorescence microscopy	Oyster	24	1.7 CFU g^{-1}	25
GLSS-this study	Seawater	1.25	100 CFU mL^{-1}	This study

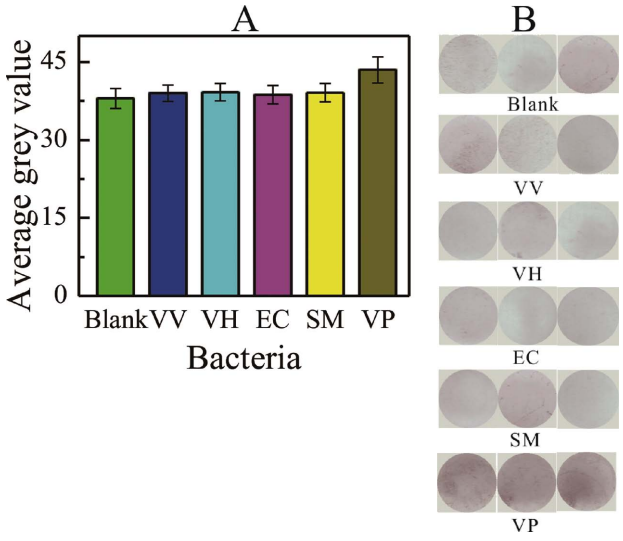

Fig. 5 Specificity of the assay. (A) Histogram of the average grey value corresponding to spot images in (B); (B) spot images of VP at the concentration of 10^2 CFU mL^{-1}, interfering bacteria (including VV, VH, EC, SM) at a concentration of 10^6 CFU mL^{-1} a and blank sample.

Meanwhile, the total assay time, 1.25 h, is less than that of most other methods. In addition, sophisticated equipment or professionals are not required, and results can be obtained visually by naked eyes. In total, the proposed GLSS method based on Christmas-tree mode can achieve rapid, inexpensive, simple and sensitive determination of VP.

Specificity stability and reproducibility of the immunosensor

To evaluate the specificity of the proposed immunosensor for VP detection, different bacteria, such as *Enterobacter cloacae* (EC) *Vibrio vulnificus* (VV), *Vibrio harveyi* (VH) and *Shewanella marisflavi* (SM) were tested (results in Fig. 5A). With the addition of VP at 10^2 CFU mL^{-1}, it could be seen that the average grey value is higher than that of VV, VH, EC and SM at 10^6 CFU mL^{-1}. As shown in Fig. 5B, it is obvious that spots of VP appear slightly darker than spots of interfering bacteria, indicating a good selectivity for VP detection.

To examine the stability and robustness of the proposed immunosensor, the AuNPs@g-C_3N_4 solution was investigated by performing the assay after storage in a refrigerator for one month at 4°C. The average grey value for the detection of 10^4 CFU mL^{-1} VP was 94.3 ± 5.3% (n = 5) of the initial value, which was obtained when the fresh detection probe solution was analyzed before storage. Thus, the results indicate that the

Table 2 Recovery tests for VP in spiked seawater and seafood samples ($\bar{x} \pm s$, $n = 5$).

Sample	Added (CFU mL^{-1})	Recovered (CFU mL^{-1})	RSD, %	Recovery, %
Seawater 1	10^3	$(1.091 \pm 0.054) \times 10^3$	4.9	109.1
Seawater 2	10^4	$(1.076 \pm 0.062) \times 10^4$	5.8	107.6
Seawater 3	10^4	$(0.943 \pm 0.043) \times 10^5$	4.6	94.3
Seawater 4	10^6	$(1.043 \pm 0.074) \times 10^6$	7.1	104.3
Seafood 1-shrimp	10^3	$(0.933 \pm 0.085) \times 10^3$	9.1	93.3
Seafood 2-fish	10^4	$(1.084 \pm 0.059) \times 10^4$	5.4	108.4
Seafood 3-shrimp	10^5	$(0.953 \pm 0.071) \times 10^5$	7.5	95.3
Seafood 4-scallop	10^6	$(0.973 \pm 0.064) \times 10^6$	6.6	97.3

sensing system is tolerant to long storage times, which is attributed to the high stability of AuNPs and g-C_3N_4.

The 10^4 CFU mL^{-1} of VP was analyzed for ten times to assess the reproducibility of this sensing system under optimal experimental conditions. The relative standard deviation (RSD) of the measurements was 6.8%, demonstrating that the reproducibility of the proposed immunosensor was excellent.

Real samples analysis

The practicality performance of the proposed method was also tested by seawater and seafood, respectively. Four levels of 10^3, 10^4, 10^5 and 10^6 CFU mL^{-1} VP were spiked to seawater and seafood samples, using the standard adding method. As shown in Table 2, satisfactory recoveries were obtained, namely, 94.3 to 109.1%, and the RSD ranged from 4.6 to 7.1% for seawater samples. The recoveries were in an acceptable range from 93.3 to 108.4%, and the RSD were in the range from 5.4 to 9.1% for seafood samples. Here, similar precision results were recorded, showing the high applications of this proposed method in practical samples.

Conclusions

In summary, this study presents a novel Christmas-tree derived immunosensor using AuNPs@g-C_3N_4 complexes and demonstrated its utility in identifying VP. Compared to the traditional direct GLSS assay, the minimal detectable concentration of VP herein was found to be as low as 10^2 CFU mL^{-1}, which is 2 orders of magnitude higher than that obtained with the traditional method. More importantly, the results can be easily visualized by naked eye, and there is no need of expensive handling, sophisticated instrument or scientific expertise. Therefore, the proposed method based on the Christmas-tree mode has the potential to become an excellent platform for VP determination in real-time. Furthermore, it should also be possible to extend this immunosensor to other targets as well by choosing other specific antibodies.

Acknowledgements

Financial support from the National Natural Science Foundation of China (41576098, 81273130, and 511601370), the Science and Technology Department of Zhejiang Province of China (2016C33176, 2016R405068), the Natural Sciences Foundation of Guangdong Province of China (2014A030313590) and Shenzhen Science and Technology Bureau (JCYJ20140508155916417) are gratefully acknowledged. This work is also sponsored by K. C. Wong Magna Fund in Ningbo University.

Supporting Information

This material is available free of charge on the Web at http://www.jsac.or.jp/analsci/.

References

1. W. Mala, M. Alam, S. Angkititrakul, S. Wongwajana, V. Lulitanond, S. Huttayananont, and C. Chomvarin, *Infec. Genet. Evol.*, **2016**, *39*, 212.
2. M. T. Hossain, Y. O. Kim, and I. S. Kong, *Mol. Cell. Probe*, **2013**, *27*, 171.
3. J. Wei, X. Zhou, D. Xing, and B. Wu, *Food Chem.*, **2010**, *123*, 852.
4. B. Bisha, J. Simonson, M. Janes, K. Bauman, and L. D. Goodridge, *Int. J. Food Sci. Tech.*, **2012**, *47*, 885.
5. C. C. Li, Z. C. Ye, L. Y. Wen, F. K. Zhao, and J. Y. Pan, *Vaccine*, **2014**, *32*, 6115.
6. Y. Hara-Kudo and S. Kumagai, *Epidemiol. Infect.*, **2014**, *142*, 2237.
7. K. S. Shaw, A. R. Sapkota, J. M. Jacobs, and B. C. Crump, *Environ. Int.*, **2015**, *74*, 99.
8. O. Laczka, M. Labbate, and M. Doblin, *Anal. Methods*, **2014**, *6*, 2020.
9. W. Jiang, X. Han, Q. Wang, and C. Ding, *Appl. Microbiol. Biot.*, **2014**, 98, 4937.
10. B. K. Kumar, P. Raghunath, D. Devegowda, V. K. Deekshit, M. N. Venugopal, and I. Karunasagar, *Int. J. Food Microbiol.*, **2011**, *145*, 244.
11. Y. R. Kim, E. Y. Kim, D. G. Kim, Y. O. Kim, M. T. Hossain, and I. S. Kong, *Anal. Biochem.*, **2012**, *424*, 32.
12. E. Sloan, M. O'Neill, C. Kaysner, A. DePaola, J. L. Nordstrom, and J. Sofos, *J. Rapid Meth. Aut. Mic.*, **2003**, *11*, 297.
13. N. Miwa, M. Kashiwagi, F. Kawamori, T. Masuda, Y. Sano, M. Hiroi, and H. Kurashige, *J. Food Hyg. Soc. Jpn.*, **2006**, *47*, 41.
14. J. L. Jones, Y. Hara-Kudo, J. A. Krantz, R. A. Benner, and A. DePaola, *Food Microbiol.*, **2012**, *30*, 105.
15. P. He, Z. Chen, J. Luo, H. Wang, and W. Gao, *Mol. Cell Probe*, **2014**, *28*, 246.
16. F. Zhao, D. Q. Zhou, H. H. Cao, and Y. H. Jiang, *Food Control*, **2011**, *22*, 1095.
17. Z. Zhang, L. Xiao, Y. Lou, M. Jin, and Y. Zhao, *Food Control*, **2015**, *51*, 31.
18. A. Tyagi, V. Saravanan, and I. Karunasagar, *Int. J. Food Microbiol.*, **2009**, *129*, 124.
19. G. Xiang, X. Pu, D. Jiang, L. Liu, C. Liu, and X. Liu, *PLOS ONE*, **2013**, *8*, e72342.
20. C. D. Tian, Y. Z. Zhang, X. Y. Ma, and J. Wang, *J. Food Safety*, **2011**, *31*, 371.
21. L. Wang, L. Shi, J. Su, Y. Ye, and Q. Zhong, *Gene*, **2013**, *515*, 421.
22. Q. Zhong, J. Tian, B. Wang, and L. Wang, *Food Control*, **2016**, *63*, 230.
23. Y. Ye, H. Li, Q. Wu, L. Na, and Y. Han, *J. Food Safety*, **2014**, *34*, 21.
24. Y. Sha, X. Zhang, W. Li, W. Wu, S. Wang, Z. Guo, J . Zhou, and X. Su, *Talanta*, **2016**, *147*, 220.
25. H. C. Chen and T. C. Chang, *Int. J. Food Microbiol.*, **1996**,

29, 311.
26. S. R. Ahmed, S. Oh, R. Baba, H. Zhou, S. Hwang, J. Lee, and E. Y. Park, *Nanoscale Res. Lett.*, 2**016**, *11*, 1.
27. T. Ding, A. W. Rudrum, L. O. Herrmann, V. Turek, and J. J. Baumberg, *Nanoscale*, **2016**, *8*, 15864.
28. Ł. Lentka, M. Kotarski, J. Smulko, U. Cindemir, Z. Topalian, C. G. Granqvist, R. Calavia, and R. Ionescu, *Talanta*, **2016**, *160*, 9.
29. L. Nie, J. Tang, H. Guo, H. Chen, P. Xiao, and N. He, *Anal. Sci.*, **2004**, *20*, 461.
30. R. Q. Liang, C. Y. Tan, and K. C. Ruan, *J. Immunol. Methods*, **2004**, *285*, 157.
31. H. J. Qi, S. H. Chen, M. L. Zhang, H. Shi, and S. Q. Wang, *Anal. Bioanal. Chem.*, **2010**, *398*, 2745.
32. Y. Deng, L. Tang, G. Zeng, J. Wang, Y. Zhou, J. Wang, J. Tang, Y. Liu, B. Peng, and F. Chen, *J. Mol. Catal. A*, **2016**, *421*, 209.
33. Z. Huang, F. Li, B. Chen, and G. Yuan, *RSC Adv.*, **2015**, *5*, 14027.
34. E. Z. Lee, S. U. Lee, N. S. Heo, G. D. Stucky, Y. S. Jun, and W. H. Hong, *Chem. Commun.*, **2012**, *48*, 3942.
35. Y. Bai, P. Q. Wang, J. Y. Liu, and X. J. Liu, *RSC Adv.*, **2014**, *4*, 19456.
36. X. Li, Z. Guo, J. Li, Y. Zhang, H. Ma, X. Pang, B. Du, and Q. Wei, *Anal. Chim. Acta,* **2015**, *854*, 40.
37. Q. Liu, Y. Guo, Z. Chen, Z. Zhang, and X. Fang, *Appl. Catal. B*, **2016**, 183, 231.
38. S. Chen, A. Li, L. Zhang, and J. Gong, *Anal. Chim. Acta*, **2015**, *896*, 68.
39. L. Du, Y. Wang, Z. Ren, C. Shen, and G. Luo, *Ind. Eng. Chem. Res.*, **2016**, *55*, 6783.
40. L. Chen, X. Zeng, P. Si, Y. Chen, Y. Chi, D. H. Kim, and G. Chen, *Anal. Chem.*, **2014**, *86*, 4188.
41. Z. Zhang, C. Chen, and X. S. Zhao, *Electroanalysis*, **2009**, *21*, 1316.
42. W. Wang, W. Y. Wu, X. Zhong, W. Wang, Q. Miao, and J. J. Zhu, *Biosens. Bioelectron.*, **2011**, *26*, 3110.